HHS Public Access

Author manuscript

*Cardiovasc Toxicol*. Author manuscript; available in PMC 2020 October 01.

Published in final edited form as:

*Cardiovasc Toxicol*. 2019 October ; 19(5): 401–411. doi:10.1007/s12012-019-09507-y.

# TOXIC EFFECTS OF PARTICULATE MATTER DERIVED FROM DUST SAMPLES NEAR THE DZHIDINSKI ORE PROCESSING MILL, EASTERN SIBERIA, RUSSIA

**Katherine E. Zychowski**[1], **Abigail Wheeler**[1], **Bethany Sanchez**[1], **Molly Harmon**[1], **Christina R. Steadman Tyler**[2], **Guy Herbert**[1], **Selita N. Lucas**[1], **Abdul-Mehdi Ali**[3], **Sumant Avasarala**[3], **Nitesh Kunda**[1], **Paul Robinson**[4], **Pavan Muttil**[1], **Jose M. Cerrato**[3], **Barry Bleske**[5], **Olga Smirnova**[6], **Matthew J. Campen**[1]

[1]Department of Pharmaceutical Sciences, University of New Mexico-Health Sciences Center, Albuquerque, NM 87131, USA

[2]Bioscience Division, Los Alamos National Laboratories, Los Alamos, NM 87545, USA

[3]Department of Civil Engineering, University of New Mexico, Albuquerque, NM 87131, USA

[4]Southwest Research and Information Center, Albuquerque, NM 87196, USA

[5]Pharmacy Practice and Administrative Sciences, University of New Mexico-Health Sciences Center Albuquerque, NM 87131, USA

[6]Geological Institute, Siberian Branch, Russian Academy of Sciences, Russia

## Abstract

Ambient particulate matter (PM) is associated with increased mortality and morbidity, an effect influenced by the metal components of the PM. We characterized five sediment samples obtained near a tungsten-molybdenum ore-processing complex in Zakamensk, Russia for elemental composition and PM toxicity with regard to pulmonary, vascular, and neurological outcomes. Elemental and trace metals analysis of complete sediment and $PM_{10}$ (the respirable fraction, <10 μm mass mean aerodynamic diameter) were performed using inductively coupled plasma optical emission spectrometry (ICP-OES) and mass spectrometry (ICP-MS). Sediment samples and $PM_{10}$ consisted largely of silicon and iron and silicon and sodium, respectively. Trace metals including manganese and uranium in the complete sediment, as well as copper and lead in the $PM_{10}$ were observed. Notably, metal concentrations were approximately 10X higher in the $PM_{10}$ than in the sediment. Exposure to 100 μg of $PM_{10}$ via oropharyngeal aspiration in C56BL/6 mice resulted in pulmonary inflammation across all groups. In addition, mice exposed to 3 of the 5 $PM_{10}$ samples exhibited impaired endothelial-dependent relaxation, and correlative analysis revealed associations between pulmonary inflammation and levels of lead and cadmium. A tendency for elevated cortical *ccl2* and *Tnf-α* mRNA expression was induced by all samples and significant upregulation was noted following exposure to $PM_{10}$ samples Z3 and Z4, respectively. Cortical *Nqo1* mRNA levels were significantly upregulated in mice exposed to $PM_{10}$ Z2. In conclusion, pulmonary

**Corresponding Authors:** Matthew J. Campen, MSC09 53601, University of New Mexico, Albuquerque, NM 87131, 505 925-7778, mcampen@salud.unm.edu.

exposure to PM samples from the Zakamensk region sediments induced varied pulmonary and systemic effects that may be influenced by elemental PM composition. Further investigation is needed to pinpoint putative drivers of neurological outcomes.

**Keywords**

cardiovascular; toxicology; neuroinflammation; particulate matter; respiratory toxicology; PM10

## 1. Introduction

Particulate matter (PM) air pollution is a major contributor to a wide breadth of health outcomes, including cardiovascular and respiratory diseases, as well as adverse birth outcomes and neurological syndromes (Brook *et al.*, 2002; Campbell *et al.*, 2005; Dominici *et al.*, 2006; Kleinman *et al.*, 2008; Brook *et al.*, 2010; Sapkota *et al.*, 2012; Keil *et al.*, 2016). PM is a heterogeneous mixture consisting of varied chemical components depending on the origin and metal content has been associated with cardiopulmonary toxicity (Campen *et al.*, 2001; Kodavanti *et al.*, 2001; Campen *et al.*, 2002; Lippmann *et al.*, 2006; Niu *et al.*, 2013; Haberzettl *et al.*, 2014) and overall morbidity and mortality (Dominici *et al.*, 2007; Bell *et al.*, 2009). Despite extensive investigations into the influence of metallic species on PM toxicity, pulmonary and vascular effects from mine-derived sediment are relatively unstudied. A recent study indicated that uranium mine site proximity is directly correlated with increased circulatory inflammation markers (Harmon *et al.*, 2017) suggesting that windblown contaminants may be an important factor in cardiopulmonary health for affected regions.

The Zakamensk region, adjacent to the Russia-Mongolia border, has an extensive legacy of metal mining, in particular for tungsten and molybdenum (Timofeev *et al.*, 2016). One recent soil survey indicated that heavy metal and metalloid pollution is prominent in the area and soils are enriched with high levels of cadmium (Cd), lead (Pb), tungsten (W), bismuth (Bi), and molybdenum (Mo) (Kasimov *et al.*; Ubugunov *et al.*, 2014). Environmental quality in this region has rapidly deteriorated due to urbanization, hasty mining operations and deforestation, and windblown transport of metal contaminants is currently among the most important pollution issues in central/eastern Asia (Yoo and Kim, 2008). A recent 3-year survey of the nearby Selenga River Basin indicated high levels of manganese (Mn), iron (Fe), chromium (Cr), copper (Cu) and arsenic (As) in surface waters, which may be due to runoff or Aeolian transport. Surface water heavy metal concentrations tend to be higher on the Mongolian side in almost all border geographic locales, with the exception of Zakamensk (Nadmitov *et al.*, 2015).

A complete profile of health effects from exposure to these mining sediments are unknown in this region, however current epidemiological evidence suggests that the relative risk of respiratory disease in the contaminated regions in children is 1.9–2.4 fold higher than the rest of the surrounding area (Imetkhenov *et al.*, 2015). The current study seeks to address concerns of Zakamensk residents about the potential for adverse human health impacts from the tens of millions of tons of uncovered, fine-particle mill tailings left on or in fields and

streams next to apartments and homes in Zakamensk by the Dzhidinskii Ore Processing Kombinat when it ceased operation (Smirnova *et al.*, 2013). As a first step, we collected sediments from 5 areas around the Zakamensk regions, isolated the PM10 fraction, characterized the elemental composition of the PM10, and conducted a battery to in vivo toxicological assessments.

## 2. Methods

### 2.1 Fractionation

Complete sediment samples were resuspended in air and collected in the Next Generation Impactor (NGI, model 170 NGI, MSP Corporation, Shoreview, MN) fitted with a pre-separator and gravimetric cups to obtain a PM respirable fraction for analysis and exposure. The size range of PM used in oropharyngeal aspiration studies was 0.75 μm−12 μm ($d_{ae}$, mass median aerodynamic diameter) with a median size of ~ 4 μm, (operationally defined as $PM_{10}$). These particulates were collected and used for subsequent animal studies. Samples were weighed and manually loaded into the hydroxypropyl methylcellulose capsules (VCaps®, size 3, Capsugel, USA). A total of 10 capsules, each containing 100 mg of powder, were filled. Each capsule was placed in an Aerolizer® and the sample was drawn through the induction port using a pump (Copley Scientific, Nottingham, UK) operated at a flow rate of 60 L/min for 4–6 s. Following aerosolization, powder deposition on each stage was determined gravimetrically.

### 2.2 PM Metals Analysis

Sample filters were cut into small pieces including attached particulates based on the measured area of the PM filters. Each sample was placed in 50 mL digestion (Digi tubes) tubes and digested at 95 °C using 2 mL nitric acid, 3 mL hydrochloric acid, and 2 mL hydrofluoric acid for 2 h. A blank (unused PM filter) was also digested as a baseline. Samples were then cooled, brought to 25 mL final volume filtered, and transferred to ICP-MS autosampler tubes for analysis.

The PerkinElmer NexION 300D ICP-MS was optimized using a mixture standard of light, medium, and heavy masses (Li, Be, Mg, In, Pb, and U). Indium (In) element was used as internal standard to monitor matrix effect. The instrument was calibrated using a blank and three standards and quality control samples were used to validate the calibration and instrument stability. Samples were analyzed in automated mode, data were validated, verified, and reported in Excel format. Inductively coupled plasma-optical emission spectrometry (ICP-OES) (PerkinElmer, Akron, OH) with a detection limit of <0.5 mg $L^{-1}$ and inductively coupled plasma-mass spectrometry (ICP-MS) (PerkinElmer, Akron, OH) with a detection limit of <0.5 $\mu$g $L^{-1}$ were used to assess the elemental composition of original sediment and $PM_{10}$ samples.

### 2.3 Animals

C57BL/6J mice (male, 6–8 weeks of age) were purchased from Jackson Laboratory (Bar Harbor, ME) and housed in an Association for Assessment and Accreditation of Lab Animal Care (AALAC)-approved facility through the University of New Mexico Health Sciences

Center. United States Public Health Service (PHS) Policy on Humane Care and Use of Laboratory Animals (Silverman *et al.*, 2014) were used as guidelines. Additionally, all procedures were approved by the Institutional Animal Care and Use Committee at the University of New Mexico. Mice were subjected to an acclimatization period of one week prior to exposure and maintained on a 12 hr light/dark cycle throughout the study with food and water provided *ad libitum*.

Mice were acutely treated via oropharyngeal aspiration with mine site-derived $PM_{10}$ (n=8 per group) prepared using physiological dispersion media (DM) as a vehicle. Dispersion media consisted of mouse serum albumin (0.6 mg/ml) and 1,2-dipalmitoyl-sn-glycero-3-phosphocholine (DCCP, 10 μg/ml) in phosphate-buffered saline (PBS). For each of the five $PM_{10}$ samples, 100 μg of was resuspended in 50 μl of DM and subsequently sonicated for 5 min to ensure adequate dispersion. Mice were randomly assigned to one of six different treatment groups, DM (vehicle control), Z1, Z2, Z3, Z4, and Z5. Twenty-four hours following aspiration, mice were euthanized under 1.5–2% isofluorane via cardiac puncture. Serum and tissues were then collected and either flash frozen and stored at −80 °C (for qPCR) or used directly (for bioassays).

## 2.4 Bronchoalveolar Lavage

Following euthanasia, bronchoalveolar lavage was performed by puncturing the trachea and intubating each mouse with a 20 gauge cannula. A total of 1 mL of PBS was injected and brochoalveolar lavage fluid (BALF) was pulled from the lungs following inflation. Total BALF cells and neutrophils were counted using trypan blue staining and a hemocytometer. BALF was centrifuged at 500 × *g* for 10 minutes at 4°C and supernatant s were analyzed for total protein using Bradford's assay (Bradford, 1976). Coomassie Brilliant Blue stain was read at an absorbance of 595 nm using a Tecan plate reader (Tecan, Mannedorf, Switzerland).

## 2.5 Force-tension myography

Thoracic aorta rings were isolated from C57BL/6 mice following acute exposure to $PM_{10}$ samples, cleaned of connective tissue, and force-transducer myography was used to examine contractile response to serotonin. Thoracic aorta ring segments (2–3 mm in length) were mounted onto a myograph system and submerged in physiological salt solution (119.0 mM NaCl, 25 mM $NaHCO_3$, 5.5 mM glucose, 4.7 mM KCl, 1.2 mM $MgSO_4$, 1.2 mM $KH_2PO_4$, 0.027 mM EDTA, and 2.5 mM $CaCl_2$). Carbagen was bubbled into the wells at 37° C with 21% $O_2$ - 5 % $CO_2$ balance $N_2$ and aortic rings were left to equilibrate at 2 g of tension for 30 min. Tension was gradually increased in 2mN increments to an optimal passive tension of 10 mN. Vessel viability was confirmed using a contractile response to the addition of PSS containing potassium (64.9 mM NaCl, 25.0 mM $NaHCO_3$, 5.5 mM glucose, 58.9 mM KCl, 1.2 mM $MgSO_4$, 1.2 mM $KH_2PO_4$, 0.027 mM EDTA, and 2.5 mM $CaCl_2$) was repeated twice to constrict the vessel. After a 30 min equilibration period, vessels were gradually constricted with increasing levels of serotonin ($10^{-9}$-$10^{-5}$ μM).

To test endothelial cell dysfunction due to circulating serum factors following $PM_{10}$ exposure, naïve aortic rings (*i.e.*, obtained from unexposed mice) were incubated in an organ

bath with serum from exposed mice for 30 min. Vessels were incubated with 1% serum obtained from mice previously exposed to DM vehicle control or $PM_{10}$ Z1–Z5 samples (n = 8 per group). Cumulative concentration-response curves to acetylcholine (Ach) were produced after the force response to serum had plateaued. ACh concentrations ($10^{-9}$-$10^{-5}$) were added to the wells every five minutes in increasing concentrations. Data were obtained using a MacLab/4e analogue-digital convertor displayed through Chart™ software (AD Instruments, USA) and calculated as a percentage of serum-induced contraction with baseline tension subtracted.

### 2.6 Gene Expression Analysis

Transcriptional analysis was performed using quantitative polymerase chain reaction (qPCR) based on previously published methods (Aragon *et al.*, 2017). Briefly, a Qiagen RNeasy Mini Kit was used to extract RNA from the right cortex. One μg of RNA was reverse-transcribed using random hexamers (Applied Biosystems) and SuperScript III (Invitrogen). Gene expression was determined using 9μL cDNA on a 96-well plate format using a StepOne real-time PCR system (Applied Biosystems). Transcriptional responses for inflammatory (*Ccl2, Il-6, and Tnf-α*) and oxidative stress (*Hmox1, Nqo1*, and *Nrf2*) markers were measured using TaqMan probes and primers (Applied Biosystems). Hypoxanthine guanine phosphoribosyltransferase (*Hprt1*) was used as an internal reference. Relative gene expression was calculated using the $2^{-\Delta\Delta Ct}$ comparative threshold method and TATA binding protein (TBP) was used as the internal control gene (Livak and Schmittgen, 2001). Exposed groups were compared to DM vehicle control mice, which served as the reference group (n=6 per group).

### 2.7 Statistics

GraphPad Prism Software (v6.0) was utilized for the analysis of pulmonary, vascular and neuroinflammatory analysis (GraphPad Prism, La Jolla, CA). Normal distributions of data were confirmed prior to statistical testing. For all graphs, data are represented as mean ± SEM. Lavage and transcriptional outcomes were compared using one-way analysis of variance (ANOVA) with Dunnett's posthoc testing. Vasomotor studies were analyzed by a repeated measures two-way ANOVA with a Fisher's Least Squared Differences approach to identify concentrations of ACh or serotonin at which trends were significantly different from DM control. Values were considered statistically significant at $p \leq 0.05$.

## 3 Results

### 3.1 Sediment Sample Collection and PM Fraction Preparation

The five sediment samples analyzed in this study were collected from locations in and around the city of Zakamensk by the Siberian Branch of the Geological Institute at the Russian Academy of Sciences and the Buryat Regional Union. Zakamensk is located in the western part of the Republic of Buryatia, Russia, on a tributary to Lake Baikal. This area is of particular interest as it lies adjacent to the Dzhidinskii Kombinat, a tungsten-molybdenum mining and milling complex in operation from the 1930's to 1991 (Fig. 1). Size distribution of the PM samples assessed using laser diffraction (Fig. 2) provided confirmation of PM ≤

10 μm. The distribution of $PM_{10}$ size in all 5 samples was very uniform, owing to the design and collection efficiencies of the NGI.

### 3.2 Original Sediment and $PM_{10}$ Elemental Characterization

For most elements, there was a high degree of similarity between the 5 samples, including both original sediment and PM fractions (Fig. 3). Elemental composition of the sediment revealed that silicon (Si), manganese (Mn), sodium (Na) and Pb were prominent components throughout Z1–Z5 samples (Fig. 3). The primary composition of the sediment consisted of Si and iron (Fe) in the >10 μm fraction and Na and Si in the <10 μm fraction (Fig. 3a, 3c). The trace metals consist of a significant amount of Mn, and uranium (U) in the >10 μm fraction and copper (Cu) and Pb in the <10 μm fraction (Fig. 3b, 3d). Among the groups, elemental composition in the Z3 group had the greatest concentration of Pb and Cd in the trace metal $PM_{10}$ group, while Z5 demonstrated the highest amount of chromium (Cr) (Fig. 3, 4). Trace element concentrations differed from original sediment with respect to variability between sample groups, which was greater in the $PM_{10}$ group across Z1–Z5 (Fig. 4).

### 3.2 Acute Pulmonary Toxicity

At 100 μg/mouse aspirations, all $PM_{10}$ samples induced some degree of inflammation and injury in the lungs. However, this effect was significantly greater in the Z3 sample (Fig. 5). The Z3 sample was the only one that significantly induced greater total cells in the BALF, relative to controls. All samples induced a degree of neutrophilia in the lavage, but the Z3 sample was significantly greater than all other samples. Total protein in the BALF was significantly elevated in the Z1 and Z3 samples relative to control. Correlational analysis revealed that the Pb and Cd components most significantly associated with the pulmonary outcomes. Neutrophil influx associated with $PM_{10}$ Pb levels ($R^2$=0.97, p=0.002) and Cd levels ($R^2$=0.92, p=0.009). Although not as statistically robust, lavage protein levels were similarly correlated with Pb ($R^2$=0.74, p=0.061) and Cd levels ($R^2$=0.79, p=0.044) (Sup. Table 1 and 2).

### 3.3 Vasomotor Effects

Aortas isolated from $PM_{10}$-treated mice were contracted with increasing doses of serotonin in an isolated organ bath preparation. Net contraction in mice treated with DM was approximately 157% of potassium-induced contractions. Aortas from mice aspirated with samples Z1 and Z2 generated significantly greater contraction in response to serotonin (Fig. 6). No effects were observed for the other three samples. Based on the metal composition, serotonin response most significantly correlated with aluminum levels ($R^2$=0.86, p=0.023) (Sup. Table 1 and 2).

Aortic rings contracted approximately 6 mN in response to the serum treatment; no difference in the magnitude of contraction was observed across exposure groups. Once contractions stabilized, increasing concentrations of acetylcholine were administered to the organ bath. Aortic rings incubated with serum from vehicle control-treated mice exhibited a mean net relaxation of 54%, consistent with several other studies using this approach (Fig. 6) (Aragon *et al.*, 2016). Significant impairments in the vasorelaxation response were

observed in the presence of serum from mice treated with the Z1, Z3, and Z5 samples, as compared to control (Fig. 7). The magnitude of impairment associated negatively with $PM_{10}$ potassium ($R^2$=0.93, p=0.008) and sodium ($R^2$=0.94, p=0.007) content (Sup. Table 1 and 2).

### 3.4 Neuroinflammation and Oxidative Stress Markers

To investigate whether exposure to mine-derived particular matter resulted in adverse neurological outcomes, the mRNA expression of cortical neuropeptides critically involved in neuroinflammation and oxidative stress were analyzed. While increasing trends were generally noted for *Ccl2, Il-6, and Tnf-α*, mRNA expression in mice exposed to $PM_{10}$ compared to DM control, however no consistent responses were seen in inflammation or oxidative stress outcomes across all samples (Fig. 8). Significant mRNA elevations were observed for *Ccl2* (induced by Z3), *Tnf-α* (induced by Z4), and *Nqo1* (induced by Z2), while oxidative stress response genes *Nrf2* and *Hmox1* remained unchanged regardless of treatment group. These significant differences in mRNA expression did not coincide with PM elemental composition.

## 1. Discussion

Metals have been understood to be major drivers of PM toxicity since work in the late 1990's on residual oil fly ash (ROFA) and Utah Valley dusts (Dye *et al.*, 2001). A series of biochemical and cellular analyses performed on rats following oropharyngeal aspiration of ROFA containing high levels of soluble transition metals established that nickel (Ni), iron (Fe) and vanadium (V) were key drivers of pulmonary (Costa and Dreher, 1997; Dreher *et al.*, 1997) and cardiovascular outcomes (Campen *et al.*, 2001; Campen *et al.*, 2002). Similar studies further noted that Ni, Fe, and V had a greater impact on pulmonary outcomes in various ROFA samples, however levels of Pb and Cd were not reported (Kodavanti *et al.*, 1998). The Utah Valley dusts, collected before, during, and after the closure of an open-hearth steel mill, were assessed for pulmonary toxicity in a manner similar to that of the present study, albeit in rats (Dye *et al.*, 2001). PM obtained during the years when the steel mill was open (1986 and 1988) contained far greater metal content and exhibited far greater pulmonary toxicity than PM collected during the temporary closure (1987) during a labor strike. While Pb was a predominant component of that PM, zinc actually appeared to align with toxic potency more closely.

Cd and Pb stood out as possible drivers of $PM_{10}$-induced lung toxicity in the present study, although overall the elemental composition and resultant toxicity of the 5 samples varied minimally. Both Cd and Pb have previously been identified as putative enhancers of adverse PM health effects. Wu and colleagues noted that cadmium was one of four metals that consistently trended with reduced lung function in a small cohort of young male subjects (Wu *et al.*, 2013). In toxicological studies, Cd has been shown to enhance PM toxicity, in terms of lung histopathological changes (Bajpai *et al.*, 1993; Wu *et al.*, 2013). The Z3 sample was the most frequently potent in terms of pulmonary, vascular, and neuroinflammatory endpoints, which by association implicates those metals, Cd and Pb, that are in greatest concentration relative to other samples. The Z3 samples were obtained just south of and most proximal to the major mine tailings pile (Fig. 1). However, our analysis

did not include other crucial factors for PM toxicity, including morphometry, surface area or zeta potential. Thus, ascribing the increased toxic potency of Z3 samples to the elemental metals composition, much less any origin related to the mine tailings, remains unproven.

Serum-borne circulating factors have been implicated in vascular dysfunction including atherosclerosis progression in several studies (Cung *et al.*, 2015; Paffett *et al.*, 2015; Aragon *et al.*, 2016; Christophersen *et al.*, 2016; Zychowski *et al.*, 2016; Aragon *et al.*, 2017). Christophersen et al. 2016 reported that PM exposure may induce bioactive serum mediators that drive vascular and systemic toxicity (Christophersen *et al.*, 2016). This study found nanoparticle-induced atherosclerotic plaque progression from 8.53 or 25.6 μg nanosized carbon black (CB) in apolipoprotein E knockout (*ApoE*$^{-/-}$) mice was accelerated following pulmonary inflammation. Aortic rings from naïve mice were incubated with serum from previously exposed ApoE$^{-/-}$ animals resulting in enhanced vasoconstriction, an effect mitigated upon treatment with serotonin receptor antagonist Ketanserin. Several studies from our laboratory have reported similar results, indicating that serum from PM-exposed animals results in inhibition of Ach-mediated vasorelaxation based on aortic force-transduced myography (Aragon *et al.*, 2015; Cung *et al.*, 2015; Aragon *et al.*, 2016; Aragon *et al.*, 2017). Additionally, the serum-cumulative inflammatory potential (SCIP) assay has revealed that serum from PM-exposed mice exhibits greater mRNA expression than control serum when incubated with endothelial cells (Aragon *et al.*, 2017). Accordingly, serotonin-treated aortas from the $PM_{10}$ sample Z1 exposed mice exhibited significantly greater aortic contraction compared to vehicle control (Fig. 6). Furthermore, Ach-mediated vasorelaxation was significantly inhibited in serum-treated aortas compared to vehicle control in the Z1, Z3 and Z5 groups. These results suggest that serum-borne factors are mediating vascular toxicity following aspiration of mining-derived PM.

Recent studies into the etiology of neurological disorders have pinpointed increased neuroinflammation and oxidation as key events in the onset and progression of diseases of the central nervous system (CNS). Particulate matter is a potent inducer of inflammation and oxidative stress and a growing body of evidence supports a direct link between pulmonary metals exposure and neurotoxicity (Campbell *et al.*, 2009; Levesque *et al.*, 2011; Levesque *et al.*, 2013; Liu *et al.*, 2016; Woodward *et al.*, 2017), Campbell et al. demonstrated that short-term exposure to air pollution increases inflammatory cytokine gene expression, including *Il-1a* and *Tnf-a*, in the CNS of BALB/c mice, an effect that was magnified in ApoE$^{-/-}$ mice (Campbell et al., 2005; Campbell et al., 2005). Pulmonary exposure to diesel exhaust particles (DEP), a major component of airborne PM, induces microglial activation and generalized neuroinflammation in rats (Levesque et al., 2009; Levesque et al., 2011), while re-aerosolized air pollution-derived nano PM exacerbates cerebral ischemia and increases inflammation and oxidative stress in the damaged region (Liu et al., 2016). Our findings recapitulate the general trend of neuroinflammation, in terms of elevated Ccl2 and Tnf-a mRNA levels, but the effect was inconsistent and modest, occurring only in the Z3 and Z4 samples, respectively. Additionally, chronic exposure to air pollution is increasingly recognized as a source of reactive oxygen species (ROS) production and a major driver of central nervous system (CNS) disease. High levels of free radicals along with decreased cerebral levels of detoxifying antioxidants have been linked to a multitude of neurological disorders including stroke, neurodegeneration, and Alzheimers (Peters *et al.*, 2006;

MohanKumar *et al.*, 2008) (Block and Calderón-Garcidueñas, 2009). Free radical production is increased upon inflammation and ROS mechanisms of action include Nrf2 activation and upregulation of Nrf2 downstream targets Hmox1 and NQO1. The present study found that neuroinflammatory effects were the greatest following exposure of mice to $PM_{10}$ sample Z3 containing high levels of Pb and Cd, however oxidative damage marker mRNA levels remained unchanged. Mice subjected to acute aspiration of $PM_{10}$ sample Z2, notably containing more V, Co, and Cu (known oxidative damage-inducing transition metals) than any other sample, exhibited elevated cortical *Nqo1* mRNA expression.

### Limitations

This study is limited in scope in several ways, and interpretation of results should similarly be restricted to match the descriptive study design. As a short-term, high dose study, we are unable to extrapolate to chronic health outcomes of inhaling such dusts. The objective of the study was to compare the acute toxicity and inflammatory potency of these PM samples and the moderately high dose was an essential aspect to generating a biological signal. Additionally, other characteristics such as organic or biological material, which was not fully characterized in this study, may have contributed to the observed PM toxicity. Furthermore, we did not conduct controlled administration or removal of specific metals (*i.e.*, Cd and Pb), thus our conclusions related to these metals as putative drivers are purely associative.

## Conclusions

High concentrations of $PM_{10}$ derived from dusts in the Zakamensk region induced pulmonary inflammation, systemic vascular dysfunction, and neuroinflammation in a manner that varied only modestly between samples. Elemental metal composition analysis was conducted but only explained a small amount of variability between samples. Specifically, the Z3 sample, which was notably high in Cd and Pb and also the most proximal sample to mine tailings, drove significant increases in pulmonary inflammation and incited systemic toxicity, in terms of systemic vascular dysfunction and the induction of cortical Ccl2 mRNA. Future studies to better address community-level exposures and to better control for metal compositional causation are needed.

## Supplementary Material

Refer to Web version on PubMed Central for supplementary material.

## Acknowledgements

This work has been supported by RFBR (grant № 16–05–01041) and NIEHS (ES026673). Katherine E. Zychowski received funding support from NIGMS (K12GM088021) through the ASERT-IRACDA program at UNM and NIEHS (K99ES029104). We thank Dr. Jesse Denson for editing this manuscript. A special thank you to Vladimir Belogolovov for collection of the dust samples.

The BRO-Baikal is a civil society focused on the protection of Lake Baikal and its tributaries based in Ulan-Ude, the capital of the Republic of Buryatia, Russia. Their US partner is the Southwest Research and Information Center (SRIC), is focused on human and natural resource impacts of mining including the prevention of air and water contamination from residual mining waste and remediation of mines in the arid southwestern US. This fantastic collaboration made this work possible.

## References


1. Aragon M, Erdely A, Bishop L, Salmen R, Weaver J, Liu J, Hall P, Eye T, Kodali V, Zeidler-Erdely P, 2016 MMP-9-dependent serum-borne bioactivity caused by multiwalled carbon nanotube exposure induces vascular dysfunction via the CD36 scavenger receptor. Toxicological Sciences 150, 488–498. [PubMed: 26801584]
2. Aragon MJ, Chrobak I, Brower J, Roldan L, Fredenburgh LE, McDonald JD, Campen MJ, 2015 Inflammatory and Vasoactive Effects of Serum Following Inhalation of Varied Complex Mixtures. Cardiovascular toxicology, 1–9. [PubMed: 24894912]
3. Aragon MJ, Topper L, Tyler CR, Sanchez B, Zychowski K, Young T, Herbert G, Hall P, Erdely A, Eye T, 2017 Serum-borne bioactivity caused by pulmonary multiwalled carbon nanotubes induces neuroinflammation via blood–brain barrier impairment. Proceedings of the National Academy of Sciences 114, E1968–E1976.
4. Bajpai R, Waseem M, Kaw JL, 1993 Pulmonary response to cadmium and nickel coated fly ash. Journal of environmental pathology, toxicology and oncology: official organ of the International Society for Environmental Toxicology and Cancer 13, 251–257.
5. Bell ML, Ebisu K, Peng RD, Samet JM, Dominici F, 2009 Hospital admissions and chemical composition of fine particle air pollution. American Journal of Respiratory and Critical Care Medicine 179, 1115–1120. [PubMed: 19299499]
6. Block ML, Calderón-Garcidueñas L, 2009 Air pollution: mechanisms of neuroinflammation and CNS disease. Trends in neurosciences 32, 506–516. [PubMed: 19716187]
7. Bradford MM, 1976 A rapid and sensitive method for the quantitation of microgram quantities of protein utilizing the principle of protein-dye binding. Analytical biochemistry 72, 248–254. [PubMed: 942051]
8. Brook RD, Brook JR, Urch B, Vincent R, Rajagopalan S, Silverman F, 2002 Inhalation of fine particulate air pollution and ozone causes acute arterial vasoconstriction in healthy adults. Circulation 105, 1534–1536. [PubMed: 11927516]
9. Brook RD, Rajagopalan S, Pope CA, Brook JR, Bhatnagar A, Diez-Roux AV, Holguin F, Hong Y, Luepker RV, Mittleman MA, 2010 Particulate matter air pollution and cardiovascular disease. Circulation 121, 2331–2378. [PubMed: 20458016]
10. Campbell A, Araujo JA, Li H, Sioutas C, Kleinman M, 2009 Particulate matter induced enhancement of inflammatory markers in the brains of apolipoprotein E knockout mice. Journal of Nanoscience and Nanotechnology 9, 5099–5104. [PubMed: 19928188]
11. Campbell A, Oldham M, Becaria A, Bondy SC, Meacher D, Sioutas C, Misra C, Mendez LB, Kleinman M, 2005 Particulate matter in polluted air may increase biomarkers of inflammation in mouse brain. Neurotoxicology 26, 133–140. [PubMed: 15527881]
12. Campen MJ, Nolan JP, Schladweiler MCJ, Kodavanti UP, Costa DL, Watkinson WP, 2002 Cardiac and thermoregulatory effects of instilled particulate matter-associated transition metals in healthy and cardiopulmonary-compromised rats. Journal of Toxicology and Environmental Health Part A 65, 1615–1631. [PubMed: 12396871]
13. Campen MJ, Nolan JP, Schladweiler MCJ, Kodavanti UP, Evansky PA, Costa DL, Watkinson WP, 2001 Cardiovascular and thermoregulatory effects of inhaled PM-associated transition metals: a potential interaction between nickel and vanadium sulfate. Toxicological Sciences 64, 243–252. [PubMed: 11719707]
14. Christophersen DV, Jacobsen NR, Jensen DM, Kermanizadeh A, Sheykhzade M, Loft S, Vogel U, Wallin H, Møller P, 2016 Inflammation and Vascular Effects after Repeated Intratracheal Instillations of Carbon Black and Lipopolysaccharide. PloS one 11, e0160731. [PubMed: 27571356]
15. Costa DL, Dreher KL, 1997 Bioavailable transition metals in particulate matter mediate cardiopulmonary injury in healthy and compromised animal models. Environmental Health Perspectives 105, 1053. [PubMed: 9400700]
16. Cung H, Aragon MJ, Zychowski K, Anderson JR, Nawarskas J, Roldan C, Sood A, Qualls C, Campen MJ, 2015 Characterization of a novel endothelial biosensor assay reveals increased

cumulative serum inflammatory potential in stabilized coronary artery disease patients. Journal of Translational Medicine 13, 99. [PubMed: 25890092]

17. Dominici F, Peng RD, Bell ML, Pham L, McDermott A, Zeger SL, Samet JM, 2006 Fine particulate air pollution and hospital admission for cardiovascular and respiratory diseases. JAMA 295, 1127–1134. [PubMed: 16522832]
18. Dominici F, Peng RD, Ebisu K, Zeger SL, Samet JM, Bell ML, 2007 Does the effect of PM10 on mortality depend on PM nickel and vanadium content? A reanalysis of the NMMAPS data. Environmental Health Perspectives 115, 1701. [PubMed: 18087586]
19. Dreher KL, Jaskot RH, Lehmann JR, Richards JH, Ghio JKMAJ, Costa DL, 1997 Soluble transition metals mediate residual oil fly ash induced acute lung injury. Journal of Toxicology and Environmental Health Part A 50, 285–305.
20. Dye JA, Lehmann JR, McGee JK, Winsett DW, Ledbetter AD, Everitt JI, Ghio AJ, Costa DL, 2001 Acute pulmonary toxicity of particulate matter filter extracts in rats: coherence with epidemiologic studies in Utah Valley residents. Environmental Health Perspectives 109, 395. [PubMed: 11427389]
21. Haberzettl P, Bhatnagar A, Conklin DJ, 2014 Particulate matter and oxidative stress–pulmonary and cardiovascular targets and consequences, Systems Biology of Free Radicals and Antioxidants. Springer, pp. 1557–1586.
22. Harmon ME, Lewis J, Miller C, Hoover J, Ali A-MS, Shuey C, Cajero M, Lucas S, Zychowski K, Pacheco B, 2017 Residential proximity to abandoned uranium mines and serum inflammatory potential in chronically exposed Navajo communities. Journal of Exposure Science and Environmental Epidemiology.
23. Imetkhenov A, Dorzhiev T, Maksarova D, Manketova A, 2015 Effects of technogenic pollution of the Dzhidinsky tungsten-molybdenum plant on the health of the children of Zakamensk (Republic of Buryatia). Bulletin of Buryat State University, 1–2.
24. Kasimov NS, Kosheleva NE, Timofeev IV, Ecological and Geochemical Assessment of Woody Vegetation in Tungsten-Molybdenum Mining Area (Buryat Republic, Russia). IOP Publishing, pp. 012026.
25. Keil D, Buck B, Goossens D, Teng Y, Leetham M, Murphy L, Pollard J, Eggers M, McLaurin B, Gerads R, 2016 Immunotoxicological and neurotoxicological profile of health effects following subacute exposure to geogenic dust from sand dunes at the Nellis Dunes Recreation Area, Las Vegas, NV. Toxicology and Applied Pharmacology 291, 1–12. [PubMed: 26644169]
26. Kleinman MT, Araujo JA, Nel A, Sioutas C, Campbell A, Cong PQ, Li H, Bondy SC, 2008 Inhaled ultrafine particulate matter affects CNS inflammatory processes and may act via MAP kinase signaling pathways. Toxicology Letters 178, 127–130. [PubMed: 18420360]
27. Kodavanti UP, Hauser R, Christiani DC, Meng ZH, McGee J, Ledbetter A, Richards J, Costa DL, 1998 Pulmonary responses to oil fly ash particles in the rat differ by virtue of their specific soluble metals. Toxicological Sciences 43, 204–212. [PubMed: 9710962]
28. Kodavanti UP, Schladweiler MCJ, Richards JR, Costa DL, 2001 Acute lung injury from intratracheal exposure to fugitive residual oil fly ash and its constituent metals in normoand spontaneously hypertensive rats. Inhalation Toxicology 13, 37–54. [PubMed: 11153059]
29. Levesque S, Taetzsch T, Lull ME, Johnson JA, McGraw C, Block ML, 2013 The role of MAC1 in diesel exhaust particle-induced microglial activation and loss of dopaminergic neuron function. Journal of Neurochemistry 125, 756–765. [PubMed: 23470120]
30. Levesque S, Taetzsch T, Lull ME, Kodavanti U, Stadler K, Wagner A, Johnson JA, Duke L, Kodavanti P, Surace MJ, 2011 Diesel exhaust activates and primes microglia: air pollution, neuroinflammation, and regulation of dopaminergic neurotoxicity. Environmental health perspectives 119, 1149. [PubMed: 21561831]
31. Lippmann M, Ito K, Hwang J-S, Maciejczyk P, Chen L-C, 2006 Cardiovascular effects of nickel in ambient air. Environmental health perspectives 114, 1662. [PubMed: 17107850]
32. Liu Q, Babadjouni R, Radwanski R, Cheng H, Patel A, Hodis DM, He S, Baumbacher P, Russin JJ, Morgan TE, 2016 Stroke damage is exacerbated by nano-size particulate matter in a mouse model. PLOS ONE 11, e0153376. [PubMed: 27071057]

33. Livak KJ, Schmittgen TD, 2001 Analysis of relative gene expression data using real-time quantitative PCR and the 2− ΔΔCT method. methods 25, 402–408. [PubMed: 11846609]
34. MohanKumar SMJ, Campbell A, Block M, Veronesi B, 2008 Particulate matter, oxidative stress and neurotoxicity. Neurotoxicology 29, 479–488. [PubMed: 18289684]
35. Nadmitov B, Hong S, Kang SI, Chu JM, Gomboev B, Janchivdorj L, Lee C-H, Khim JS, 2015 Large-scale monitoring and assessment of metal contamination in surface water of the Selenga River Basin (2007–2009). Environmental Science and Pollution Research 22, 2856–2867. [PubMed: 25217283]
36. Niu J, Liberda EN, Qu S, Guo X, Li X, Zhang J, Meng J, Yan B, Li N, Zhong M, 2013 The role of metal components in the cardiovascular effects of PM2. 5. PloS one 8, e83782. [PubMed: 24386277]
37. Paffett ML, Zychowski KE, Sheppard L, Robertson S, Weaver JM, Lucas SN, Campen MJ, 2015 Ozone inhalation impairs coronary artery dilation via intracellular oxidative stress: evidence for serum-borne factors as drivers of systemic toxicity. Toxicological Sciences, kfv093.
38. Peters A, Veronesi B, Calderón-Garcidueñas L, Gehr P, Chen LC, Geiser M, Reed W, Rothen-Rutishauser B, Schürch S, Schulz H, 2006 Translocation and potential neurological effects of fine and ultrafine particles a critical update. Particle and fibre toxicology 3, 13. [PubMed: 16961926]
39. Sapkota A, Chelikowsky AP, Nachman KE, Cohen AJ, Ritz B, 2012 Exposure to particulate matter and adverse birth outcomes: a comprehensive review and meta-analysis. Air Quality, Atmosphere and Health 5, 369–381.
40. Silverman J, Suckow MA, Murthy S, 2014 The IACUC handbook. CRC Press.
41. Smirnova OK, Doroshkevich CG, Dampilova BV, 2013 Assessment of trends of changes in the content of toxic elements in the soils of the city of Zakamensk after the conservation of the Dzhidnsky tungsten-molybdenum plant. Geodynamics and mineralogy of Northeast Asia Materials of the IV All-Russian Scientific and Practical Conference. Ulan-Ude: Publishing house “Ecos”, 327–330.
42. Timofeev IV, Kasimov NS, Kosheleva NE, 2016 Soil cover geochemistry of mining landscapes in the South-East of Transbaikalia (City of Zakamensk). Geography and Natural Resources 37, 200–211.
43. Ubugunov V, Dorzhonova V, Ubugunov L, 2014 Cd extraction potential of Thlaspi caerulescens in extracontinental climate conditions (Zakamensk, Buryatia, Russia). Journal of Geochemical Exploration 144, 380–386.
44. Woodward NC, Levine MC, Haghani A, Shirmohammadi F, Saffari A, Sioutas C, Morgan TE, Finch CE, 2017 Toll-like receptor 4 in glial inflammatory responses to air pollution in vitro and in vivo. Journal of neuroinflammation 14, 84. [PubMed: 28410596]
45. Wu S, Deng F, Hao Y, Shima M, Wang X, Zheng C, Wei H, Lv H, Lu X, Huang J, 2013 Chemical constituents of fine particulate air pollution and pulmonary function in healthy adults: the Healthy Volunteer Natural Relocation study. Journal of hazardous materials 260, 183–191. [PubMed: 23747477]
46. Yoo GY, Kim IA, 2008 Development and application of a climate change vulnerability index. Korea Environment Institute 2008, 1–88.
47. Zychowski KE, Sanchez B, Pedrosa RP, Lorenzi-Filho G, Drager LF, Polotsky VY, Campen MJ, 2016 Serum from obstructive sleep apnea patients induces inflammatory responses in coronary artery endothelial cells. Atherosclerosis 254, 59–66. [PubMed: 27693879]

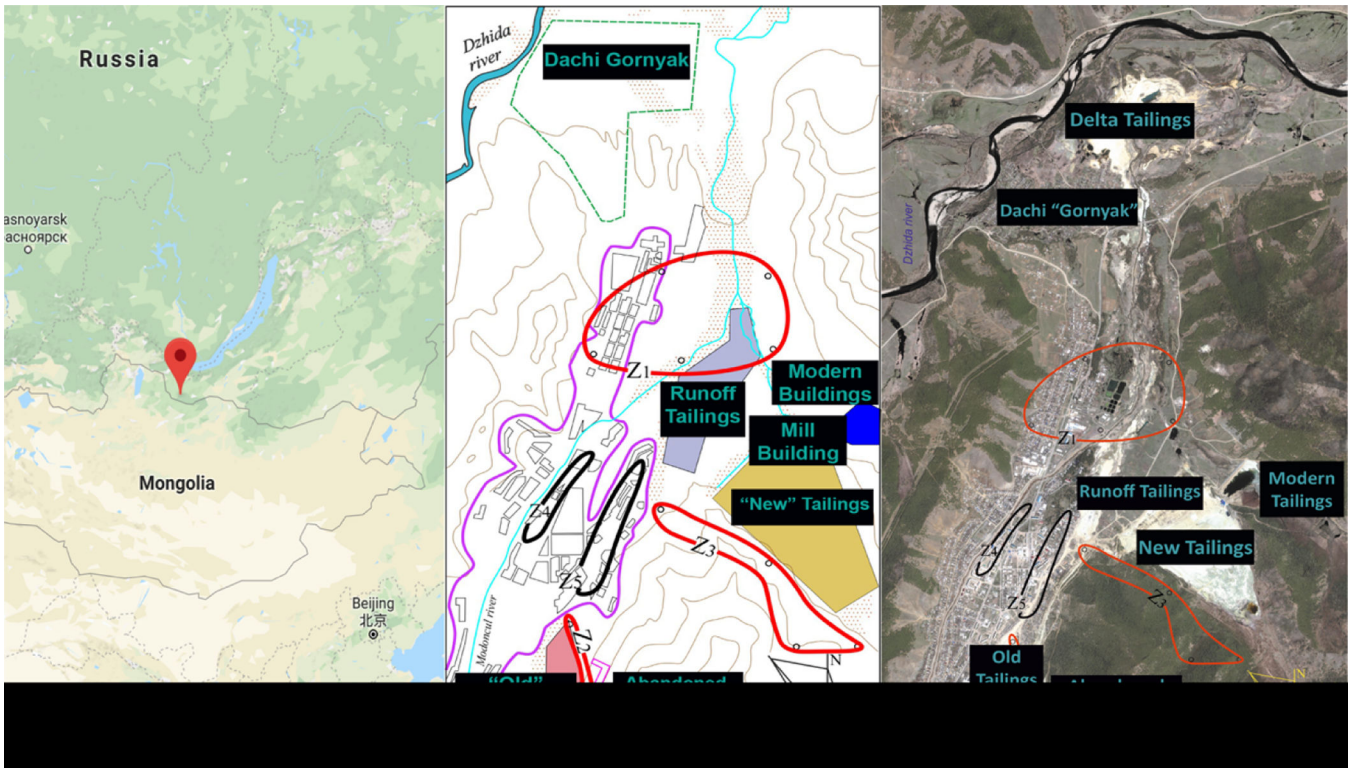


**Figure 1.**

Map showing location of Zakamensk, Russia with illustrations indicating major tailing piles Location of Zakamensk, Russia (left) immediately adjacent Mongolia and south of Lake Baikal. Simple map of Zakamensk (middle) to better illustrate regions of tailings and sampling. Satellite image of Zakamensk (right) identifying major tailings piles and Z1–Z5 areas for sediment sampling.

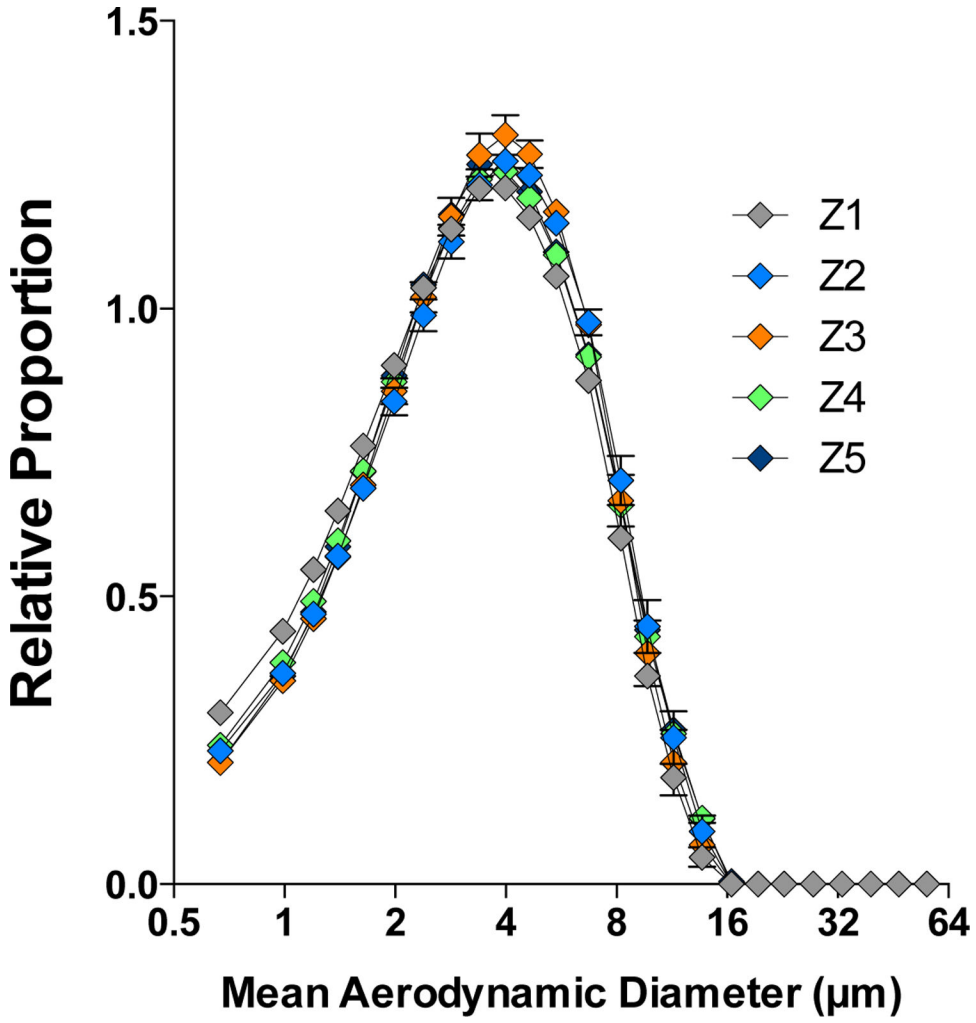


**Figure 2.**
Size distribution of PM in dispersion media suspension for mouse exposures. Samples were measured using laser diffraction spectroscopy.

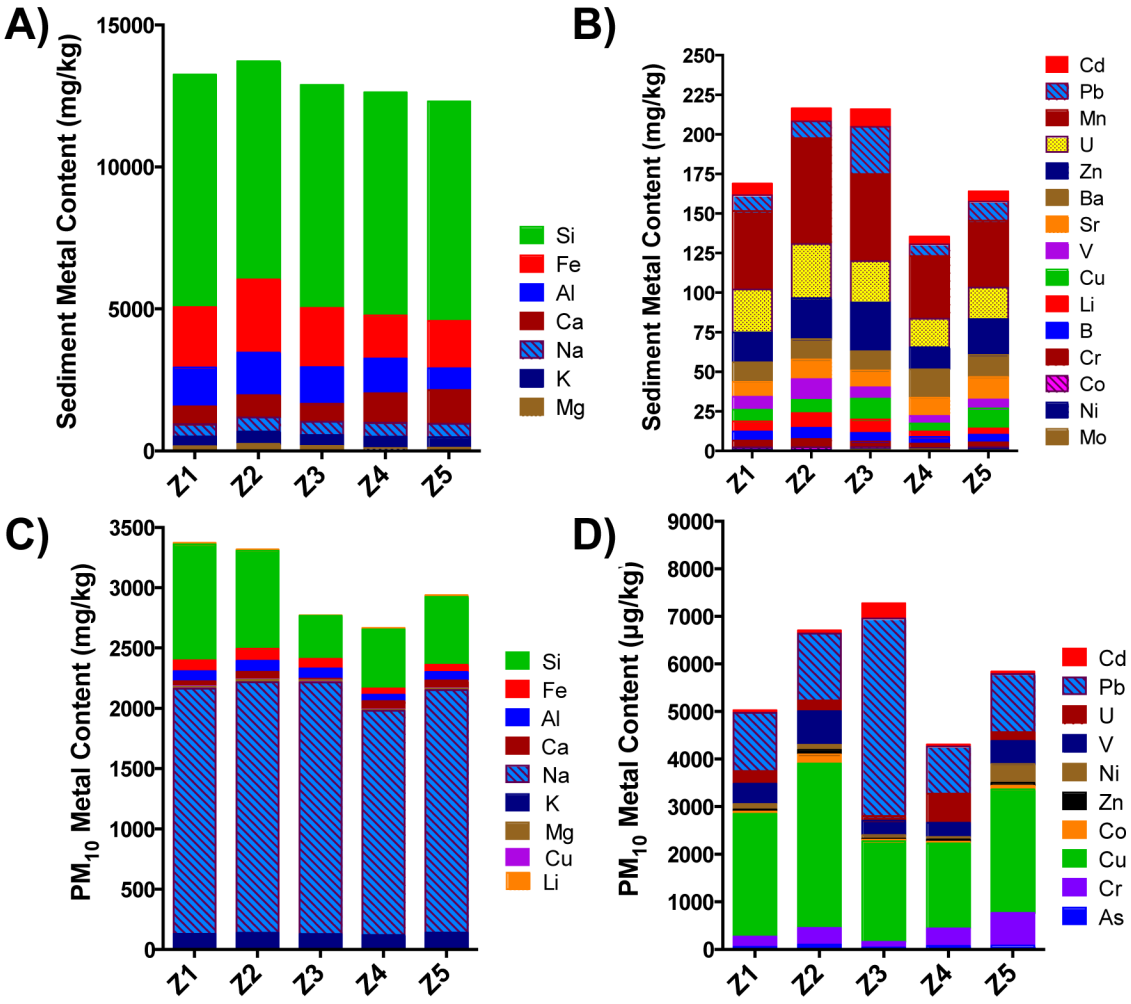


**Figure 3.**

Elemental composition of complete sediment samples Z1–Z5 (a, b) compared to the derived $PM_{10}$ samples (c,d). a and c represent the major elemental components, while b and d represent the trace metals. Concentrations were determined by ICP-OES.

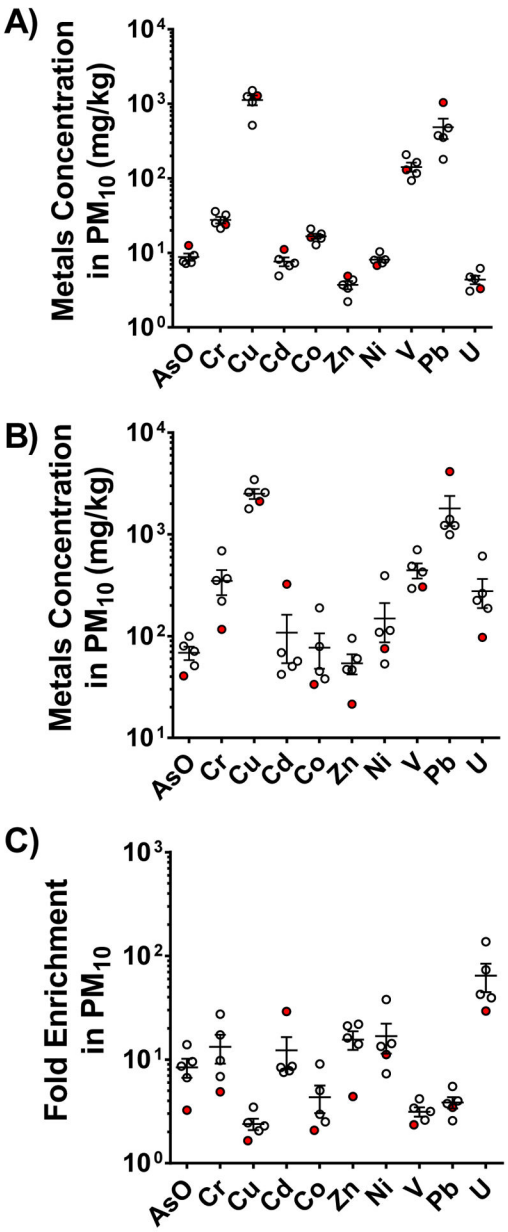


**Figure 4.**

Trace element concentrations. Original sediment (a) and $PM_{10}$ (b) fraction along with an index of enrichment, the ratio comparing original and $PM_{10}$ (c). Z3 is highlighted in red to note the clear differences in Cd and Pb levels.

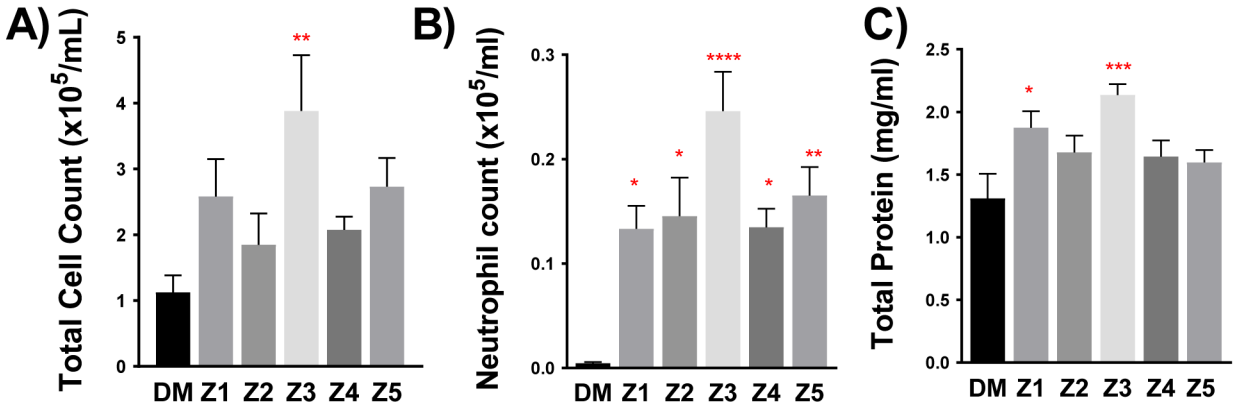


**Figure 5.**

Pulmonary inflammation and injury markers as assessed by (a) BALF total cell number (b) neutrophil influx in BALF and (c) total protein in cells isolated from BALF. Data are represented as mean ± SEM. Asterisks indicate significant difference from DM control group by one-way ANOVA using Dunnett's multiple comparison test (*p<0.05, **p<0.01; ***p<0.001; ****p<0.0001; n=7–8 per group). A Neuman-Keuls posthoc test revealed significant differences between neutrophil levels induced by Z3 compared to all other PM groups.

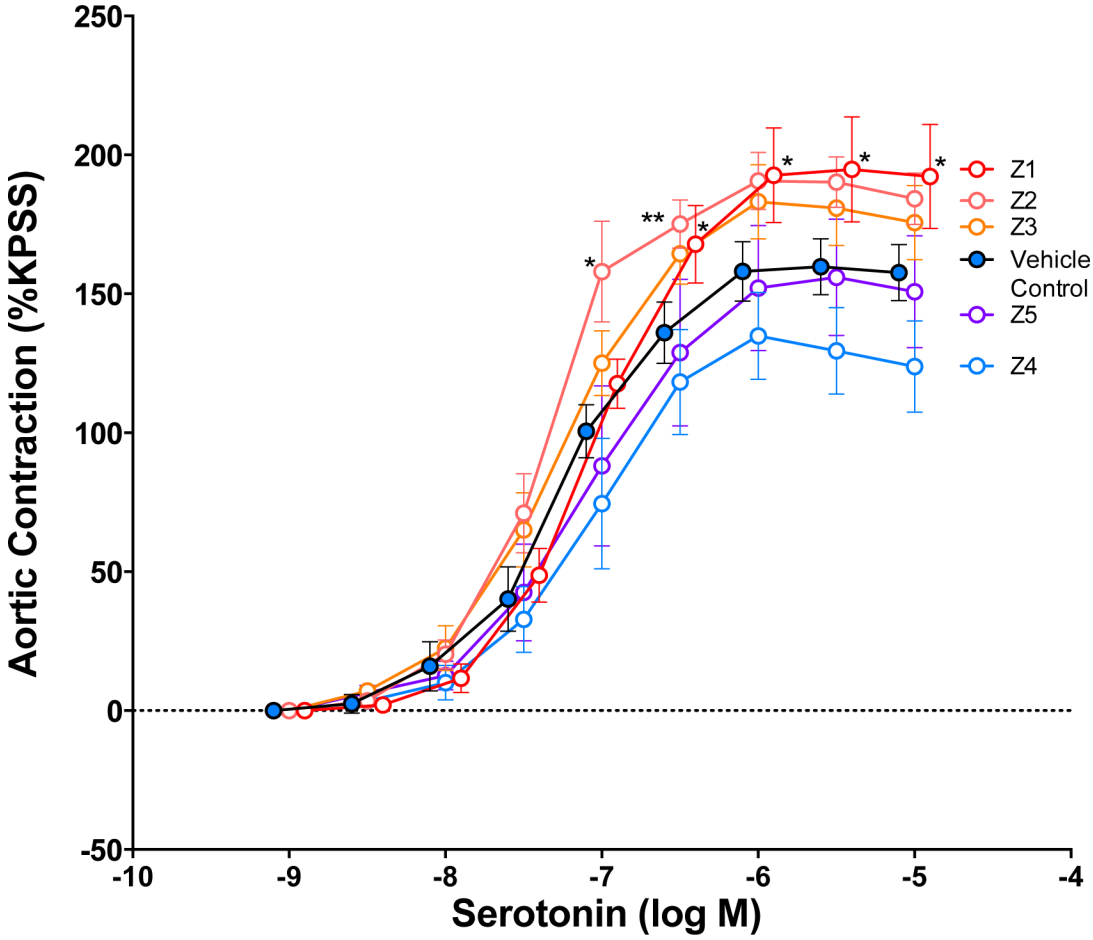


**Figure 6.**

Serotonin-induced contraction in aortic rings obtained from acutely treated DM control and $PM_{10}$ -treated mice. Data are represented as mean ± SEM. Asterisks indicate significant difference from DM control group by two-way ANOVA (p=0.038) using an Uncorrected Fisher's Least Squared Differences test (*p<0.05, **p<0.01; n=4–6 per group).

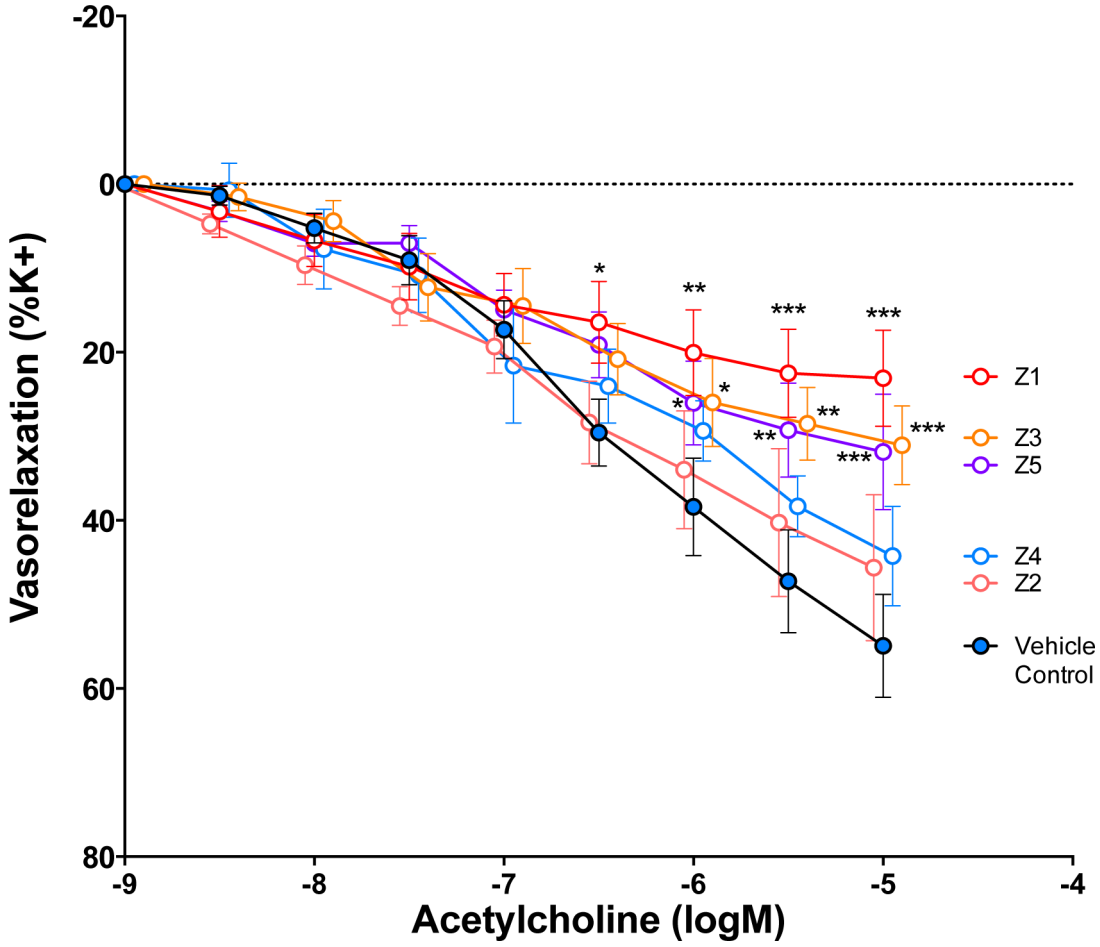


**Figure 7.**

Acetylcholine-induced vasorelaxation in naïve aortic rings treated with serum obtained from DM control and $PM_{10}$-treated mice (acute exposure). Data are represented as mean ± SEM. Asterisks indicate significant difference from DM control group by two-way ANOVA ($p<0.0001$) using an Uncorrected Fisher's Least Squared Differences test (*$p<0.05$, **$p<0.01$; ***$p<0.001$; n=4–6 per group).

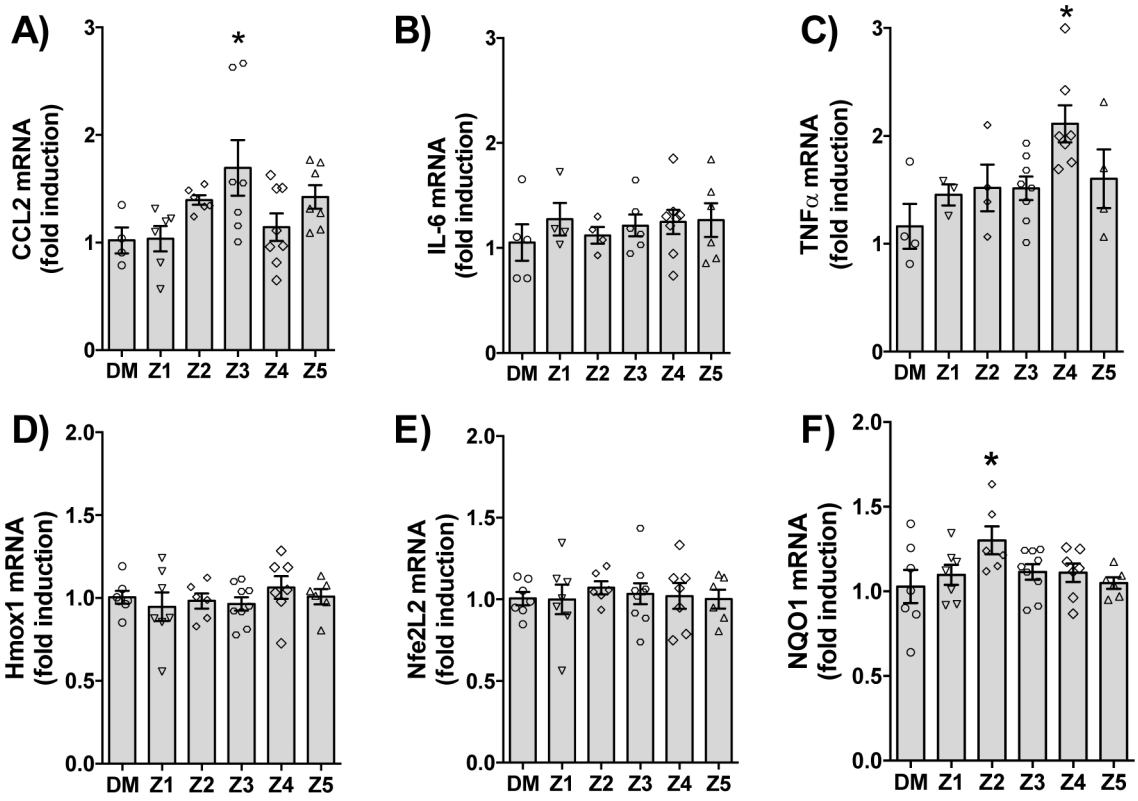


**Figure 8.**

Quantitative real-time analysis of (a) neuroinflammatory peptides and (b) oxidative stress markers in the frontal cortex following acute exposure to $PM_{10}$ sediment samples. Data are represented as mean ± SEM. Asterisks indicate significant difference compared to DM control by one-way ANOVA with Dunnett's post-hoc test (*p<0.05; **p<0.01; n= 8 per group).